Journal of Materials Chemistry C

Accepted Manuscript

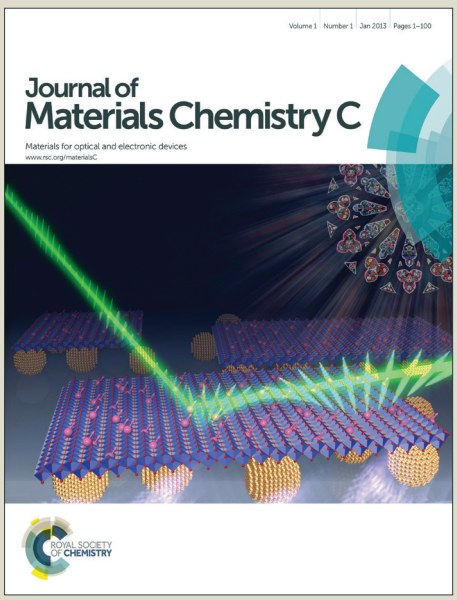

ROYAL SOCIETY OF CHEMISTRY

www.rsc.org/materialsC

Journal of Materials Chemistry C

Dynamic Article Links ►

Cite this: DOI: 10.1039/c0xx00000x

www.rsc.org/xxxxxx

Paper

Band Gap Modulation of Janus Graphene Nanosheets by Interlayer Hydrogen Bonding and External Electric Field: A Computational Study

Feng Li[a] and Yafei Li*[,a]

Received (in XXX, XXX) Xth XXXXXXXXX 20XX, Accepted Xth XXXXXXXXX 20XX

DOI: 10.1039/b000000x

In this work, density functional theory computations with van de Waals (vdW) corrections revealed the existence of rather strong C−H···F−C hydrogen bonding between hydrofluorinated graphene (HGF) monolayers, which have Janus-like geometrics. Interestingly, the individual HGF monolayer is semiconducting with a direct energy gap of 2.82 eV while HGF bilayer is metallic in its most stable stacking pattern. Especially, applying an external electric field can effectively open a band gap for HGF bilayer, and correspondingly cause a metallic-semiconducting transition. These results open opportunities in fabricating electronic and optoelectronic devices based on HGF nanosheets, and call for more usage of the weak interactions for band structure engineering.

Introduction

Janus, which is depicted to have two faces, is the god of beginnings and transitions in ancient Roman religion. In recent years, the myth of Janus also stimulated people to fabricate various nanostructures with Janus-like configuration due to the promising applications of Janus anisotropy in molecular recognition,[1] self-assembly,[2, 3] sensors,[4] and drug delivery.[5] For instance, self-assembly of molecular Janus particles based on derivatives of MNPs, fullerene and POM were used as building blocks to form structural stable two-dimensional (2D) nanocrystals,[6] which has been widely recognized as an effective "bottom-up" approach to engineer advanced functional materials.

Graphene, a single layer of graphite, has attracted considerable research attention in the past decade due to its intriguing physical properties, such as mass-less Dirac fermions, ultrahigh carrier mobility, superior thermal conductivity and high mechanical strength.[7-12] These properties endow graphene many promising applications in various fields. However, the lack of a band gap has essentially restricted the applications of graphene in macroelectronics. To conquer this problem, various approaches towards generating a band gap in graphene have been proposed and explored. Notably, it has been shown that the covalent functionalization, such as hydrogenation and fluorination, is an effective approach for the band gap opening of graphene.[13] Both experimental and theoretical studies have demonstrated that both fully hydrogenated (graphane)[14-18] and fluorinated graphene (fluorographene)[19-25] are semiconducting with rather large band gaps, and even single-sided patterned hydrogenated or fluorinated graphene also presents a large band gap (> 3 eV).[26] However, such large band gaps also restrict the wide applications of these graphene derivatives because most microelectronics and optoelectronics devices require semiconductors with no more than 3 eV band gap. Therefore, new strategies for achieving graphene materials with a moderate band gap are strongly required.

The intensive studies of Janus nanostructures inspire us to answer an interesting question: if the two sides of graphene are functionalized by H and F, respectively, what novel electronic properties can the as-obtained hydrofluorinated graphene (HGF) present? Can it have a smaller band gap than these of graphene hydrides and fluorides? Furthermore, recent studies have showed that the weak interactions not only can combine some 2D materials together, but also can modify their electronic properties significantly.[27-34] For instance, Fokin *et al.* computationally demonstrated that there is strong interlayer bonding between multilayered graphanes.[35] Li *et al*. demonstrated that the novel CH/π interaction between graphene and partially hydrogenated graphene can lead to the bandgap opening for graphene.[36] Li *et al.* also demonstrated that there exists considerable C−H···F−C bonding between graphane and fluorographene layers, and the graphane/fluorographene bilayer has a band gap much lower than those of individual graphane or fluorographene monolayer.[37] Inspired by these interesting studies, we wonder that whether it is possible to pair two HGF monolayer together through the interfacial weak interactions? If yes, can HGF bilayer present different electronic properties from those of HGF monolayer? To address these issues, density functional theory computations with van de Waals (vdW) corrections were performed.

In this work, we systematically investigated the structural and electronic properties of HGF monolayer and bilayer by means of vdW-corrected density functional theory computations. We demonstrated that two HGF monolayers can be paired together through considerable interfacial C−H···F−C hydrogen bonding. Interestingly, the HGF bilayer is metallic while the individual HGF monolayer is semiconducting with a direct energy gap of 2.82 eV, suggesting the possibility of tuning the electronic properties of nanomaterials via weak interactions. Moreover, we

also show that a metallic-semiconducting transition can occur in HGF bilayer by applying an external electronic field (E-field).

Computational details

Our density functional theory computations were performed using the Vienna *Ab initio* Simulation Package.[38] The projector-augmented wave (PAW) method was employed to represent the ion-electron interaction. The generalized gradient approximation (GGA) expressed by the PBE functional[39] and a 500 eV cutoff energy for the plane-wave basis set were adopted in all computations. Since standard PBE functional are unable to describe correctly weak interactions resulting from dynamical correlations between fluctuating charge distributions, we adopted a PBE-D2 (D stands for dispersion) approach with the Grimme vdW correction by adding a semi-empirical dispersion potential to the conventional Kohn-Sham DFT energy.[40] This approach introduces damped atom-pairwise dispersion correction of the form C_6R^{-6} in the DFT formalism. From the DFT ground state electron density and reference values of the free atoms, the C_6 coefficients and the vdW radii (R) can be directly determined. The accuracy of PBE-D2 has been well validated in recent literature.[37]

The optimizations of the lattice constants and the atom coordinates were carried out by minimizing the total energies. Cutoff energy of 500 eV is good enough for numerical convergence using 9×9×1 Monkhorst-Pack k-mesh grids. All structures were fully relaxed until the force on each atom is less than 10^{-3} eV/Å and the total energy changes are less than 10^{-5} eV. Self-consistent computations were performed with a convergence criterion of 10^{-6} eV in energy. For the density of states (DOS) computations, 15×15×1 k-point grids were employed.[41, 42] We set the x and y directions parallel and the z direction perpendicular to the layer planes, and adopted a vacuum space 25 Å in the z direction to prevent the interaction effect from neighbouring cells.

Results and discussion

Structural and Electronic Properties of HGF Monolayer. The first question is which is the most stable conformation for HGF monolayer? Similar to graphane and fluorographene, HGF has three possible conformers, *viz*., chair, boat, and stirrup. In the chair and boat conformers, H and F atoms alternates singly and in pairs on both sides of the graphene sheet, respectively,[43, 44] while in the stirrup conformer, three consecutive H and F atoms alternate on either side of the sheet.[45, 46] For graphane and fluorographene, the chair conformers have been found to have the highest stability, while in the H and F co-grafting *h*-BN sheets,[47] the most stable structure is the stirrup conformer. As shown in Fig. 1(a), our computations showed that the chair conformer of HGF has the highest stability, which is 0.46 and 0.36 eV/unit cell lower in energy than the boat and stirrup conformers, respectively. Thus, the chair conformer was then adopted for the following HGF bilayer construction. The lattice constant of chair conformer was optimized to be 2.55 Å, which is reasonable as it lies between the lattice constants of graphane (2.54 Å[37]) and fluorographene 2.60 Å[37]). Due to the addition of H and F, all carbon atoms are tuned from sp^2 to sp^3 hybridization, and the C-H and C-F bond length are 1.11 and 1.38 Å respectively. Our computations show that the H and F co-grafting HGF monolayer has a slightly smaller direct energy gap of 2.82 eV, with the valence band maximum (VBM) and conduction band minimum (CBM) both located at the Γ point (Figure 1b). For comparison, we also calculated the electronic properties of the graphane monolayer and fluorographane monolayer, which have a wider direct energy gap of 3.44 and 3.11 eV, respectively (See ESI).

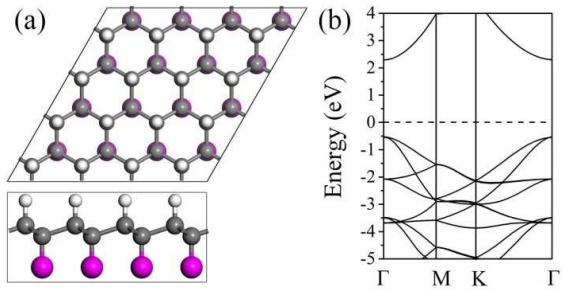

Fig. 1 (a) Top (upper) and side (bottom) views of ground state structure of HGF monolayer. (b) Electronic band structures of HGF monolayer.

Structural Properties of HGF Bilayer. Next we constructed the infinite 2D HGF bilayer by attaching two HGF monolayers together. Considering the structural properties of HGF monolayer, two HGF monolayer can be paired together through C-H···F-C, C-H···H-C, or C-F···F-C interaction. To identify which type of interlayer interaction is energetically favourable for HGF bilayer, for each stacking pattern we performed a set of lateral shifts of one HGF monolayer to the basal plane of the other and got several stable configurations. The most stable configuration for each stacking pattern are displayed in Fig. 2 while the meta-stable configurations are displayed in Fig. S1.

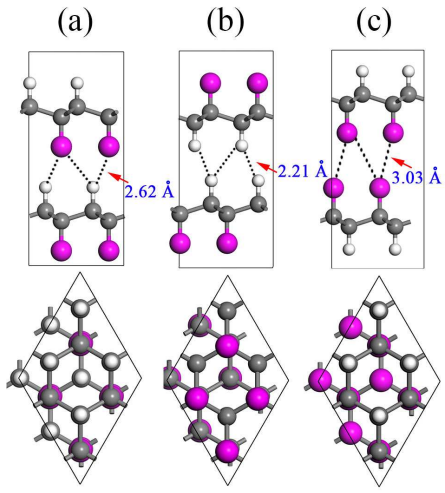

Fig. 2 Side (upper) and top (bottom) views of the most stable structure of HGF bilayer for (a) C-H···F-C, (b) C-H···H-C, and (c) C-F···F-C interaction, respectively. The ground state structure favors the C-H···F-C bonding type.

Our computations revealed that the most stable configuration of HGF bilayer favors the C-H···F-C interaction with one F (or H) atom of one HGF monolayer points to the centre site of three H (or F) atoms on the other HGF monolayer. The binding energy of C-H···F-C bilayer is 126 meV/unit cell, while the binding energies of C-H···H-C and C-F···F-C bilayers are 54 and 22

meV/unit cell, respectively. These results reflect the stronger strength of C-H···F-C interaction than that of C-H···H-C or C-F···F-C interaction. Considering the bonding strength, the C-H···F-C and C-H···H-C interactions can be seen as hydrogen bonding while the C-F···F-C interaction is mainly of vdw interaction. Computed at the same PBE-D2 theoretical level, the binding energy of the energetically most favourable HGF bilayer (126 meV/unit cell) is larger than that of graphene bilayer (106 meV/unit cell), but slightly lower than that of *h*-BN bilayer (139 meV/unit cell). For comparison, the binding energies of graphane bilayer (82 meV/unit cell) and fluorographane bilayer (73 meV/unit cell) were also calculated, which are much lower than that of HGF bilayer. The above results indicate that the C-H···F-C hydrogen bonding between HGF bilayer is a strong enough to combine two HGF monolayers together.

Why there exists so strong interfacial C–H···F–C hydrogen bonding in HGF bilayer? According to Bader charge population analysis, there is about 0.024 |e|/unit cell charge transfer from the bottom HGF monolayer to upper HGF monolayer, resulting in a spontaneous interlayer polarization in the direction from upper layer to bottom layer. This is a direct evidence for the bridge role of C-F···H-C bonding in the electron transfer between the HGF monolayers. Actually, this charge redistribution is a nature of hydrogen bonding systems, which could lead to relatively strong interaction between HGF monolayers.

Electronic Properties of HGF Bilayer. To explore the effect of interfacial C-H···F-C hydrogen bonding on the electronic properties of the HGF bilayer, we calculated the band structure and the density of states (DOS) of HGF bilayer, which are shown in Fig. 3(a). As a comparison, the electronic properties of graphane bilayer and fluorographane bilayer were also calculated (see ESI).

To match two HGF monolayers together, the elongation of lattice constant by 0.6 % further slightly increases the energy gap of individual HGF from ground state of 2.82 to 2.89 eV. However, when two HGF monolayers are paired together by C-H···F-C hydrogen bonding, a remarkable modification occurs in the band structure of HGF bilayer. As shown in Fig. 3(a), the computed band structure shows that HGF bilayer is metallic, with an energy level crossing the Fermi level. In sharp contrast, the band gap of graphane bilayer (3.50 eV) and fluorographene bilayer (2.97 eV) are quite close to those of monolayered graphane (3.44 eV) and fluorographene (3.11 eV). Moreover, considering that the standard GGA functionals systematically underestimates band gaps of semiconducting materials, we also computed the band gaps of HGF bilayer as well as monolayer by using the HSE06 hybrid functional for validation. The HSE06 band gap for the HGF monolayer is 4.03 eV and the HGF bilayer is still metallic, indicating that HSE06 and PBE actually predict qualitatively the same trends.

The density of states (DOS) analysis reveals that the states for valence bands close to Fermi level mainly come from the *p* orbitals bottom HGF layer, while those for conduction bands are dominantly contributed by the *p* orbitals upper HGF layer. Thus, the VBM and CBM of HGF bilayer are well separated on the bottom and upper HGF layers, respectively.

To get a better understanding of the mechanism of the band gap reduction in HGF bilayer, we calculated the partial charge densities plots of the VBM (Fig. 3(b)) and the CBM (Fig. 3(c)) at the Γ point for HGF bilayer. We clearly see that the VBM is contributed by the carbon skeleton and F atoms on the bottom HGF layer, whereas the CBM exhibits a strong delocalized feature which almost comes from the carbon skeleton and the H atoms on the upper HGF layer. This is well consistent with the above DOS analyses. In this way, our research suggests a rather flexible way to modify the semiconducting properties of 2D materials to metallic, opening new opportunities in fabricating practical electronics and optical devices.

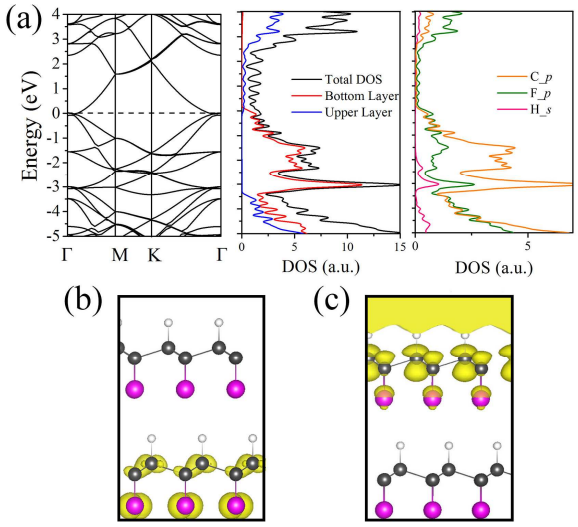

Fig. 3 (a) Electronic band structures (left) and density of states (right) of HGF bilayer. The Fermi level is assigned at 0 eV. The partial charge densities of the (b) valence band maximum (VBM) and (c) conduction band minimum (CBM) at the Γ point. The isovalue is 0.03 e/Å^3.

We also explored the effect of the interlayer polarization by calculating the plane-averaged electrostatic potential along the normal of the HGF bilayer, as plotted in Fig. 4. Clearly, a significant electrostatic potential difference was found between two HGF monolayers, as denoted by two potential wells. Compared with the bottom HGF monolayer, the electrostatic potential of the upper HGF monolayer is obviously lowered. Correspondingly, the energy levels of the upper HGF monolayer would move downwards while those on the upper monolayer would be shifted upwards, leading to the band gap closure for HGF bilayer. Therefore, the spontaneous interlayer polarization induced by the C-F···H-C hydrogen bonding should be responsible for the semiconducting-metallic transition in HGF bilayer.

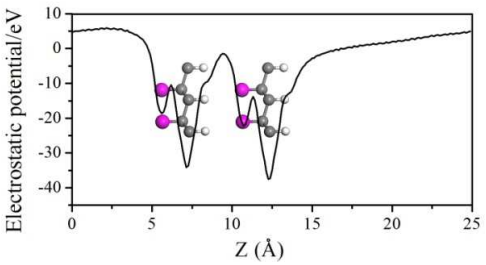

Fig. 4 Plane-averaged electrostatic potential along the HGF bilayer normal.

Effect of External E-field. Appling external E-field has proven an efficient approach toward tuning the electronic properties of many 2D materials.[48-50] Inspired by these studies, we systematically investigated the effect of the E-field on the electronic properties of HGF nanosheets. In this work, the direction of E-field is applied to be perpendicular to the plane of HGF bilayer, pointing from the bottom HGF layer to upper HGF layer (Fig. 5(a)). The band gap of HGF monolayer and bilayer as a function of E-field are both plotted in Fig. 5(b).

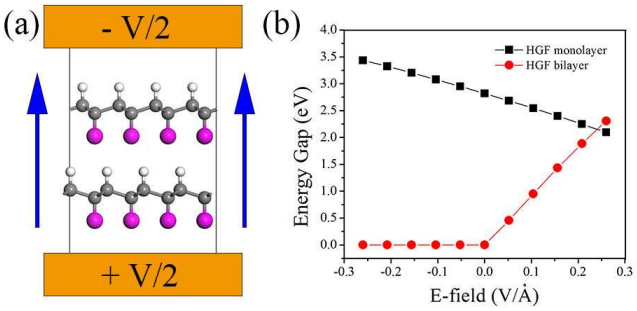

Fig. 5 (a) Schematic diagram of HGF bilayer with the E-field. The arrows denote the positive direction of the E-field. (b) Energy gap of HGF monolayer (black square) and bilayer (red circle) as a function of E-field.

Our computations show that the external E-field truly has a remarkable impact on the electronic properties for both HGF monolayer and bilayer, and HGF bilayer is more sensitive to the external E-field than HGF monolayer. For HGF monolayer, the calculated band gap shows linear reductions with the external E-field. For HGF bilayer, it keeps to be metallic under the negative electric filed; when the E-field is applied in the positive direction, the band gap increases rapidly with increasing E-filed, and can increase up to 2.31 eV at the E-field of 0.025 V/Å.

The opposite effect of the external E-field on VBM and CBM of HGF bilayer would be responsible for the metallic-semiconducting transition. With a positive E-field, the electrostatic potential on the bottom HGF monolayer is lowered while that on the upper monolayer is increased. As a result, the VBM on the bottom HGF moves downward while the CBM on the upper monolayer would be shifted upwards. This mechanism effectively opens the energy gap of HGF bilayer to semiconducting. In contrast, with a negative E-field, the potential difference between two HGF monolayer would be enlarged. Correspondingly, the VBM on the bottom layer moves continuously upward while the CBM of the upper HGF is further shifted downward, eventually keeps the HGF bilayer metallic.

Moreover, the required E-field for metallic-semiconducting transition is experimentally realizable,[51] therefore, the band gap of HGF bilayer can be efficiently tuned by the external E-field, and the metallic-semiconducting transition can be easily achieved. Although the GGA method may systematically underestimate the value of band gap, the trends of the electronic properties of HGF nanosheets subjected to external E-field predicted here should not be changed.

Conclusions

In summary, our comprehensive theoretical computations revealed considerable interactions between HGF bilayer *via* C−H···F−C hydrogen bonding. Quite different from the individual HGF monolayer that has a wide band gap of 2.82 eV, HGF bilayer is metallic, suggesting a rather flexible way toward tuning the electronic properties of 2D materials. Furthermore, HGF bilayer can be efficiently tuned from metallic to semiconducting under an experimental reliable E-field. Considering the recent progress in synthesizing 2D Janus materials[52,53] and self-assembly of graphene materials, we are optimistic that HGF nanosheets can be realized experimentally sooner.

Acknowledgements

This work was supported by NSFC of China Grant No. 21403115, Jiangsu Specially Appointed Professor Plan, and the Priority Academic Program Development of Jiangsu Higher Education Institutions. The computational resources utilized in this research were provided by Shanghai Supercomputer Center.

Notes and references

[a] *College of Chemistry and Materials Science, Jiangsu Key Laboratory of Biofunctional Materials, Nanjing Normal University, Nanjing 210023, China; E-mail: liyafei.abc@gmail.com*

† Electronic Supplementary Information (ESI) available: [Possible stacking patterns for HGF bilayer and the electronic properties of graphane monolayer and bilayer, fluorographane monolayer and bilayer]. See DOI: 10.1039/b000000x/

1. A. Walther and A. H. E. Muller, *Chem. Rev.*, 2013, 113, 5194-5261.
2. V. Percec, P. Leowanawat, H. J. Sun, O. Kulikov, C. D. Nusbaum, T. M. Tran, A. Bertin, D. A. Wilson, M. Peterca, S. D. Zhang, N. P. Kamat, K. Vargo, D. Moock, E. D. Johnston, D. A. Hammer, D. J. Pochan, Y. C. Chen, Y. M. Chabre, T. C. Shiao, M. Bergeron-Brlek, S. Andre, R. Roy, H. J. Gabius and P. A. Heiney, *J. Am. Chem. Soc.*, 2013, 135, 9055-9077.
3. J. Yan, M. Bloom, S. C. Bae, E. Luijten and S. Granick, *Nature*, 2012, 491, 578-581.
4. M. Meilikhov, S. Furukawa, K. Hirai, R. A. Fischer and S. Kitagawa, *Angew. Chem. Int. Ed.*, 2013, 52, 341-345.
5. H. Xie, Z. G. She, S. Wang, G. Sharma and J. W. Smith, *Langmuir*, 2012, 28, 4459-4463.
6. H. Liu, C. H. Hsu, Z. W. Lin, W. P. Shan, J. Wang, J. Jiang, M. J. Huang, B. Lotz, X. F. Yu, W. B. Zhang, K. Yue and S. Z. D. Cheng, *J. Am. Chem. Soc.*, 2014, 136, 10691-10699.
7. A. K. Geim and K. S. Novoselov, *Nat. Mater.*, 2007, 6, 183-191.
8. K. S. Novoselov, A. K. Geim, S. V. Morozov, D. Jiang, Y. Zhang, S. V. Dubonos, I. V. Grigorieva and A. A. Firsov, *Science*, 2004, 306, 666-669.
9. P. R. Wallace, *Phys. Rev.*, 1947, 71, 622-634.
10. R. R. Nair, P. Blake, A. N. Grigorenko, K. S. Novoselov, T. J. Booth, T. Stauber, N. M. R. Peres and A. K. Geim, *Science*, 2008, 320, 1308-1308.
11. J. S. Bunch, A. M. Zande, S. S. Verbridge, I. W. Frank, D. M. Tanenbaum, J. M. Parpia, H. G. Craighead and P. L. McEuen, *Science*, 2007, 315, 490-493.
12. M. Pumera, *The Chemical Record*, 2009, 9, 211-223.
13. D. C. Elias, R. R. Nair, T. M. G. Mohiuddin, S. V. Morozov, P. Blake, M. P. Halsall, A. C. Ferrari, D. W. Boukhvalov, M. I. Katsnelson, A. K. Geim and K. S. Novoselov, *Science*, 2009, 323, 610-613.
14. K. E. Whitener, W. K. Lee, P. M. Campbell, J. T. Robinson and P. E. Sheehan, *Carbon*, 2014, 72, 348-353.
15. R. Balog, B. Jorgensen, L. Nilsson, M. Andersen, E. Rienks, M. Bianchi, M. Fanetti, E. Laegsgaard, A. Baraldi, S. Lizzit, Z. Sljivancanin, F. Besenbacher, B. Hammer, T. G. Pedersen, P. Hofmann and L. Hornekaer, *Nat. Mater.*, 2010, 9, 315-319.

16. S. Ryu, M. Y. Han, J. Maultzsch, T. F. Heinz, P. Kim, M. L. Steigerwald and L. E. Brus, *Nano Lett.*, 2008, 8, 4597-4602.
17. Z. Q. Luo, T. Yu, K. J. Kim, Z. H. Ni, Y. M. You, S. Lim, Z. X. Shen, S. Z. Wang and J. Y. Lin, *ACS Nano*, 2009, 3, 1781-1788.
18. M. H. F. Sluiter and Y. Kawazoe, *Phys. Rev. B*, 2003, 68, 085410.
19. R. R. Nair, W. Ren, R. Jalil, I. Riaz, V. G. Kravets, L. Britnell, P. Blake, F. Schedin, A. S. Mayorov, S. Yuan, M. I. Katsnelson, H. M. Cheng, W. Strupinski, L. G. Bulusheva, A. V. Okotrub, I. V. Grigorieva, A. N. Grigorenko, K. S. Novoselov and A. K. Geim, *Small*, 2010, 6, 2877-2884.
20. L. T. Zhang, L. X. Chen, X. Z. Xiao, X. L. Fan, J. Shao, S. Q. Li, H. W. Ge and Q. D. Wang, *Int. J. Hydrogen Energy*, 2014, 39, 12715-12726.
21. C. B. Sun, Y. Y. Feng, Y. Li, C. Q. Qin, Q. Q. Zhang and W. Feng, *Nanoscale*, 2014, 6, 2634-2641.
22. N. A. Nebogatikova, I. V. Antonova, V. Y. Prinz, V. B. Timofeev and S. A. Smagulova, *Carbon*, 2014, 77, 1095-1103.
23. M. S. Zhu, X. D. Xie, Y. L. Guo, P. L. Chen, X. W. Ou, G. Yu and M. H. Liu, *Phys. Chem. Chem. Phys.*, 2013, 15, 20992-21000.
24. D. K. Samarakoon, Z. F. Chen, C. Nicolas and X. Q. Wang, *Small*, 2011, 7, 965-969.
25. K. J. Jeon, Z. Lee, E. Pollak, L. Moreschini, A. Bostwick, C. M. Park, R. Mendelsberg, V. Radmilovic, R. Kostecki, T. J. Richardson and E. Rotenberg, *ACS Nano*, 2011, 5, 1042-1046.
26. D. Haberer, C. E. Giusca, Y. Wang, H. Sachdev, A. V. Fedorov, M. Farjam, S. A. Jafari, D. V. Vyalikh, D. Usachov, X. J. Liu, U. Treske, M. Grobosch, O. Vilkov, V. K. Adamchuk, S. Irle, S. R. P. Silva, M. Knupfer, B. Buchner and A. Gruneis, *Adv. Mater.*, 2011, 23, 4497.
27. S. Lebegue, J. Harl, T. Gould, J. G. Angyan, G. Kresse and J. F. Dobson, *Phys. Rev. Lett.*, 2010, 105, 196401.
28. V. Barone, O. Hod, J. E. Peralta and G. E. Scuseria, *Acc. Chem. Res.*, 2011, 44, 269-279.
29. L. Spanu, S. Sorella and G. Galli, *Phys. Rev. Lett.*, 2009, 103, 196401.
30. Y. J. Dappe, M. A. Basanta, F. Flores and J. Ortega, *Phys. Rev. B*, 2006, 74, 205434.
31. Z. H. Zhang, W. L. Guo and B. I. Yakobson, *Nanoscale*, 2013, 5, 6381-6387.
32. Q. Tang, Z. Zhou, P. W. Shen and Z. F. Chen, *ChemPhysChem*, 2013, 14, 1787-1792.
33. A. Ramasubramaniam, D. Naveh and E. Towe, *Phys. Rev. B*, 2011, 84, 205325.
34. Q. H. Liu, L. Z. Li, Y. F. Li, Z. X. Gao, Z. F. Chen and J. Lu, *J. Phys. Chem. C*, 2012, 116, 21556-21562.
35. A. A. Fokin, D. Gerbig and P. R. Schreiner, *J. Am. Chem. Soc.*, 2011, 133, 20036-20039.
36. Y. Li and Z. Chen, *J. Phys. Chem. C*, 2012, 116, 4526-4534.
37. Y. F. Li, F. Y. Li and Z. F. Chen, *J. Am. Chem. Soc.*, 2012, 134, 11269-11275.
38. G. Kresse and J. Furthmuller, *Phys. Rev. B*, 1996, 54, 11169-11186.
39. J. P. Perdew, K. Burke and M. Ernzerhof, *Phys. Rev. Lett.*, 1996, 77, 3865.
40. S. Grimme, *J. Comput. Chem.*, 2007, 27, 1787-1799.
41. D. O. Scanlon, A. Walsh and G. W. Watson, *Chem. Mater.*, 2009, 21, 4568-4576.
42. D. O. Scanlon and G. W. Watson, *Chem. Mater.*, 2009, 21, 5435-5442.
43. W. Chen, Y. F. Li, G. T. Yu, C. Z. Li, S. B. B. Zhang, Z. Zhou and Z. F. Chen, *J. Am. Chem. Soc.*, 2010, 132, 1699-1705.
44. J. Zhou, Q. Wang, Q. Sun and P. Jena, *Phys. Rev. B*, 2010, 81, 085442.
45. J. Berashevich and T. Chakraborty, *Phys. Rev. B*, 2009, 80, 033404.
46. A. Bhattacharya, S. Bhattacharya, C. Majumder and G. P. Das, *Phys. Rev. B*, 2011, 83, 033404.
47. A. Bhattacharya, S. Bhattacharya, C. Majumder and G. P. Das, *Phys Status Solidi-RRL*, 2010, 4, 368-370.
48. F. Wu, Y. Liu, C. Yu, D. Shen, Y. Wang and E. Kan, *J. Phys. Chem. Lett.*, 2012, 3, 3330-3334.
49. E. J. Kan, F. Wu, H. J. Xiang, J. L. Yang and M. H. Whangbo, *J. Phys. Chem. C*, 2011, 115, 17252-17254.
50. Y. F. Li and Z. F. Chen, *J. Phys. Chem. C*, 2014, 118, 1148-1154.
51. Y. B. Zhang, T. T. Tang, C. Girit, Z. Hao, M. C. Martin, A. Zettl, M. F. Crommie, Y. R. Shen and F. Wang, *Nature*, 2009, 459, 820-823.
52. E. C. Ou, X. J. Zhang, Z. M. Chen, Y. G. Zhan, Y. Du, G. P. Zhang, Y. J. Xiang, Y. Q. Xiong, W. J. Xu, *Chem-Eur J*, 2011, 17, 8789-8793.
53. L. M. Zhang, J. W. Yu, M. M. Yang, Q. Xie, H. L. Peng, Z. F. Liu, *Nat. Commun.*, 2013, 4, 1443.

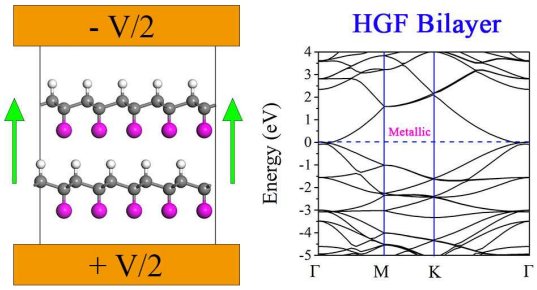

The electronic properties of hydrofluorinated graphene nanosheets can be efficiently modified by the interlayer C−H···F−C hydrogen bonding